Arabian Journal for Science and Engineering (2023) 48:16151–16165
https://doi.org/10.1007/s13369-023-08069-0

RESEARCH ARTICLE-CHEMICAL ENGINEERING

Effect of Curing Temperature on Properties of Compressed Lateritic Earth Bricks Stabilized with Natural Pozzolan-Based Geopolymer Binders Synthesized in Acidic and Alkaline Media

Rolande Aurelie Tchouateu Kamwa[1] · Sylvain Tome[1,5] · Juvenal Giogetti Deutou Nemaleu[2] · Leonel Tchadjie Noumbissie[4] · Birgit Tommes[3] · Idriss Eguekeng[1] · Alex Spieß[3] · Dennis Woschko[3] · Judicael Chongouang[1] · Christoph Janiak[3] · Marie-Annie Etoh[1]

Received: 16 January 2023 / Accepted: 13 June 2023 / Published online: 7 July 2023

Abstract
The present work aims to evaluate the curing temperatures on the engineering and structural properties of the compressed earth blocks (CEBs) produced using natural pozzolan-based acid and alkali-geopolymers as alternative binders. A fixed 15 wt% of binder made with both acid and alkaline solution and natural pozzolan was used to stabilize the laterite soils. Prior, the 7 days aged pressed samples were oven-cured at 45, 55, 65, and 75 °C for 2 days before covering and storing at room temperature for 28 days. The obtained products were subjected to physicochemical, mechanical, structural and microstructural characterizations. These include optical microscopic (OM), scanning electron microscopy/energy-dispersive X-ray spectroscopy (SEM/EDX), Fourier transform infrared spectroscopy (FTIR), powder X-ray diffraction (PXRD), percentage of water absorption, dry and wet compressive strengths, and capillary rate flow. The results revealed that the acidic binder was more efficient for the stabilization of the blocks compared to the alkaline one. The values of the dry compressive strength were 17.48, 26.50, 26.00, 25.00, and 25.00 MPa, and 9.36, 9.75, 11.64, 10.08, and 9.00 MPa at 25, 45, 55, 65, and 75 °C for the acidic binder stabilized block and alkaline binder blocks, respectively. Furthermore, at 45 and 55 °C in acid and alkaline mediums, respectively, the lowest capillary rise values of 3.30 and 6.25 for acid-stabilized and alkaline-stabilized CEBs were recorded, making this value the optimal temperature for the consolidation process during the stabilization of CEB-based lateritic using the alternative activating binder. However, curing temperatures above 45 °C for the acidic-stabilized CEBs and 55 °C for the alkaline-stabilized CEBs reduce the mechanical performance of the end products.

Keywords Lateritic soil · Natural pozzolan · Acid-geopolymer binder · Alkali-geopolymer binder · Curing temperature · Characterizations

1 Introduction

Access to affordable housing remains a major issue in both low-income and developed countries. This is reflected in Cameroon by a housing deficit ranging from the most affluent metropolis to the most remote rural areas [1, 2], owing to the exorbitant prices of modern industrial materials such as cement and steel. As a result, urban planning experts estimated an urgent need for approximately one million housing units in 2010, but with rising population over the years, this

✉ Rolande Aurelie Tchouateu Kamwa
aurelietchouateu19@gmail.com

✉ Marie-Annie Etoh
etoh_m@hotmail.com

1 Department of Chemistry, Faculty of Sciences, University of Douala, P.O. Box 24157, Douala, Cameroon

2 Local Material Promotion Authority (MIPROMALO), P.O. Box 2396, Yaoundé, Cameroun

3 Institut für Anorganische Chemie und Strukturchemie, Heinrich-Heine-Universität Düsseldorf, Universitätsstr. 1, 40225 Düsseldorf, Germany

4 Department of Civil Engineering Science, University of Johannesburg, P. O. Box. 524, Auckland Park 2006, South Africa

5 Department of Civil Engineering, University Institute of Technology (IUT), University of Douala, P. O. Box. 8698, Douala, Cameroon

figure has more than fivefold increased (to about five million units). This has prompted the government to implement new strategies such as investing in public housing construction projects in various Cameroonian communities. Despite this commendable initiative, most of the materials used in the project's execution are imported, posing issues of accessibility and cost [3]. Numerous studies are currently being conducted to reduce the cost of housing as well as pollution during the various manufacturing processes of building materials by using mainly the local feedstock for the production of durable construction materials. As a result, there is a resurgence in the use of eco-materials (such as earth and wood) for construction [4]. Earth-based materials are more commonly used in construction as raw earth bricks. One of the reasons for its use is its availability and proximity to the habitat's realization site, and it is less energy-intensive. However, when earth-based materials are not stabilized, they have disadvantages such as fast crumbling, low mechanical resistance, systematic shrinkage cracks, and especially low water absorption. Scientific studies on the stabilization of earth-based materials by hydraulic binders (Portland cement and lime) have been conducted in the literature [5]. However, the use of Portland cement (PC) causes air pollution, and its production is very energy-demanding [6, 7]. In addition, the production of this traditional cement is limited in countries with low limestone deposits and energy problems such as Cameroon. Given all of these factors, as well as the limited use of pozzolan in Cameroon construction, it is necessary to develop methods for the synthesis of construction materials that promote the use of local resources and have a low environmental impact.

Recently, several research studies have proposed geopolymer binders activated in alkaline or acidic media as an eco-efficient alternative binder to PC, especially in countries with large quantities of these volcanic wastes. Thus, the stabilization of earth bricks by this type of binder (geopolymer) with relatively low CO_2 emissions compared to Portland cement would be one of the solutions to valorize Cameroon's local potential while improving the characteristics of earth bricks [8, 9]. Furthermore, the synthesized products demonstrated good properties at slightly higher curing temperatures. In our recent work, we have shown the possibility of using 15 wt% of pozzolan-based acid geopolymer for the efficient stabilization of clay soil-based CEBs [10]. Furthermore, Weijin Wang et al. (2021) have shown the effect of curing temperature on the properties of sustainable eco-friendly unburned bricks from slate tailings. The results show that the curing temperature directly affects the mechanical performance of unburned bricks [11]. The current study thus evaluates the effect of curing temperature on CEB stabilized using acidic-based activating solution and alkaline-based activating solution as an alternative binder. This work also intends to produce sustainable construction materials with appropriate curing temperature conditions. For this purpose, the densification parameters and dry compressive strength were used to assess the main characteristics and performance properties of the stabilized bricks. Furthermore, optical microscopy (OM), scanning electron microscopy (SEM), and Fourier transform infrared spectroscopy (FTIR) were used to assess the relationship between physical and structural features.

2 Materials and Experimental Methods

2.1 Materials and Stabilization Procedures

The lateritic soil (LS) was used as a matrix of compressed bricks. LS was collected from Mangoule in the Littoral region of Cameroon. After collection, one part was used to determine water content, and the other was oven-dried at 105 °C for 24 h. Afterwards, the dried sample was ball milled and sieved through a 500-μm sieve.

Natural pozzolan (PZ) was used as a main solid precursor and was collected from a quarry located in Djoungo in the Littoral-Cameroon. After crushing, the obtained material was oven-dried at 105 °C for 48 h before ball milled, powdered, and sieved under 80 μm of size.

River sand (Sa) was used in this study to adjust the particle size distribution of the lateritic soils. Sa was collected from the Sanaga Maritime River in Littoral-Cameroon. After collection, Sa was oven-dried at 105 °C for 24 h and sieved through a 2-mm sieve.

From Table 1, the lateritic soil used is mainly composed of 22.40 wt% of SiO_2, 24.50 wt% of Al_2O_3 and 40.70 wt% of Fe_2O_3. Their corresponding particle distribution was 28.90% gravel, 20.10% of sand, 18.00% of silt, and 33.00% of clay and the plasticity index was 27.60 (Table 2). Considering the granulometry requirements of laterite for construction applications (70.00% of sand-gravel and 30.00% of clay-silt) [12], the particle size distribution of LS can be amended by sand to correct this deficiency [13, 14]. Furthermore, sand plays a key role in the volume stability of the blocks and their cost price [15]. In the present work, the use of sand was constituted of 39.80% gravel, 60.20% fine sand, and 0.80% silt (Table 2).

The main components of PZ are SiO_2 (49.90 wt.%), Al_2O_3 (15.80 wt.%), Fe_2O_3 (8.21 wt.%), and TiO_2 (12.90 wt.%) (Table 1). The presence of silicon and aluminium oxides in high percentages in PZ shows that this natural pozzolan is rich in the aluminosilicate phase and is potential precursor material for the geopolymerization reaction [16].

The crystalline phases present within both aluminosilicate raw materials are presented in Fig. 1a, b. From Fig. 1a, pozzolan powder exhibited the predominant peaks of anorthite ($CaAl_2Si_2O_8$, $2\theta = 21.95°, 27.86°$), diopside ($CaMgSi_2O_6$, $2\theta = 26.62°$), feldspar ($Na_2Al_2Si_3O_{10}$, $2\theta = 36.52°$),

Table 1 Chemical composition of pozzolan (PZ) and lateritic soil (LS)

Oxides (%)	SiO_2	Al_2O_3	Fe_2O_3	TiO_2	K_2O	MgO	P_2O_5	CaO	ZrO_2	V_2O_5	LOI
PZ	47.90	15.80	8.60	12.9	3.70	2.80	6.40	-	-	47.9	0.90
LS	22.42	24.51	40.69	1.25	0.25	0.13	0.09	0.04	0.09	0.05	10.40

Table 2 Result of particle size analysis, Atterberg limits and sand equivalent of raw materials

Particle size					
Samples	Aspect	% of gravel (ϕ > 2 mm)	% of sand (2 > ϕ > 0.02 mm)	% of silt (0.02 > ϕ > 0.002 mm)	% of clay (ϕ < 0.002 mm)
LS	Gravel lateritic	28.90	20.10	18.00	33.00
PZ	Clean sand	78.70	20.10	1.20 0	
Sa	Clean sand	39.80	60.20	0.80 0	
Atterberg limits					
	Liquidity limit	Limit of plasticity	Plasticity index	Water content	
LS	57.50	29.90	27.60	31.31	

forsterite (Mg_2SiO_4, $2\theta = 23.9°$ 29.76°), calcite ($CaCO_3$, $2\theta = 56.53°$) and magnetite with $2\theta = 35.67$ and 62.22° [13]. The presence of the dome between 20 and 35° (2θ) indicates the presence of an amorphous phase substantiating its ability to use for geopolymer synthesis [9], whereas lateritic soil powder (Fig. 1b) exhibited the predominant peaks of kaolinite (with $2\theta = 14.8°$, 25.1°, 42°, 45°, and 68°), halloysite (with $2\theta = 18°$, 28°, 36.2°, 43°), muscovite (with $2\theta = 18°$, 28°, 36.2°, and 55°), quartz (with $2\theta = 23°$, 28°, 43°, 53.2°, 60°, 68°), anatase (with $2\theta = 33.4°$), magnetite (with $2\theta = 43°$ and 63°), maghemite (36.2° and 68°) and boehmite (42° and 65°) [2, 16].

Figure 2a, b shows the infrared spectra related to chemical functional groups present within the raw materials used. For LS (Fig. 2a), the broad absorption bands observed at 3650 and 794 cm^{-1} are attributed to OH vibrations of kaolinite [17]. Those located at 3435 and 1633 cm^{-1} are assigned to H–O-H bending vibrations modes related to the presence of the water molecules. The absorption bands found at 469 and 427 cm^{-1} result from the symmetric and asymmetric vibrations of Si–O–Si bonds, indicating the presence of quartz [16]. The bands at 912 cm^{-1} is attributed to the Al(IV)–O–H and Al(VI)–O–Si bending vibration of the bonds related to the kaolin group [17, 18]. The bands at 693 and 534 cm^{-1} are the Fe–O bonds of hematite or magnetite [19].

As shown in Fig. 2b, pozzolan exhibits the bond characteristic of the asymmetric stretching vibrations of Si–O–T (T = Si or Al) with a band at 966 cm^{-1} [20, 21]. The bands at 631 and 728 cm^{-1} correspond to Si–O bending vibration [18], while the band at 569 cm^{-1} represents the vibration of Si–O–Fe bonds [22].

2.2 Stabilization of Clay Soil

Table 3 lists the details and composition of the developed stabilized blocks. Firstly, fractions of sand (10 wt%) and pozzolan (15 wt%) were added to the lateritic earth. The resultant product was manually mixed in dry state. Afterwards, this was mixed with the activating solution (alkaline solution or acid solution of 10 M concentration) having a ratio of 0.8 (solution/pozzolan) using a laboratory mortar mixer. The obtained paste was kept for 5 min to settle-down the exothermic reaction due to the dissolution of reactive phases before adding water until a malleable semi-plastic paste state. The obtained pastes were used to shape the experimental specimens by uniaxial pressing at around 8 MPa into 40 × 40 × 40 mm cubic moulds. After demoulding, the specimens were labelled and sealed with plastic covers for 7 days to initiate the geopolymerization process. After 7 days of curing, other samples were thermally activated at 45, 55, 65, and 75 °C during 48 h.

The coding system used is composed of superscript capital letters that designate the activating solution (A for acidic solution and B for alkaline solution), and X representing the curing temperature. As an example, $CEB^{B}{}_{45}$ designates a compressed earth brick formulated with an alkaline solution and a curing temperature at 45 °C.

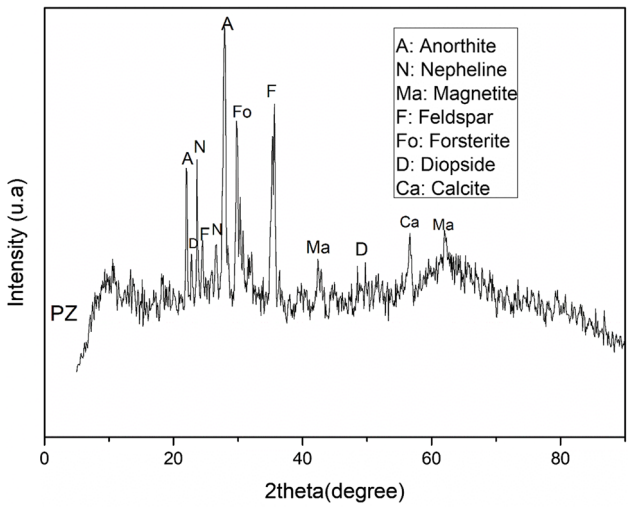

(a) Powder X-ray diffractogram of pozzolan (PZ).

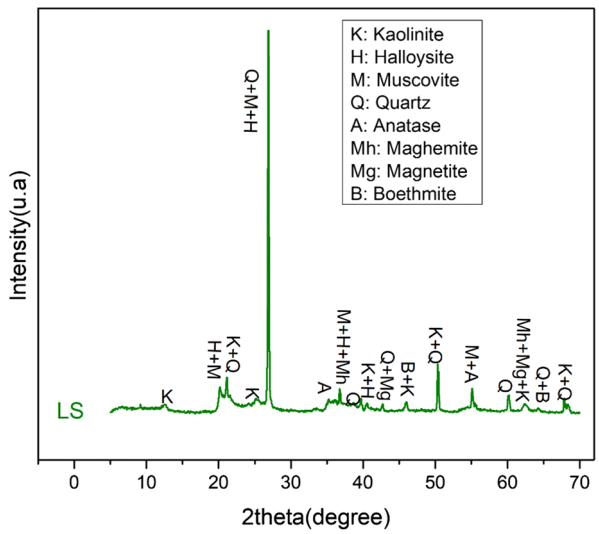

(b) Powder X-ray diffractogram of lateritic soil (LS).

Fig. 1 **a** Powder X-ray diffractogram of pozzolan (PZ). **b** Powder X-ray diffractogram of lateritic soil (LS)

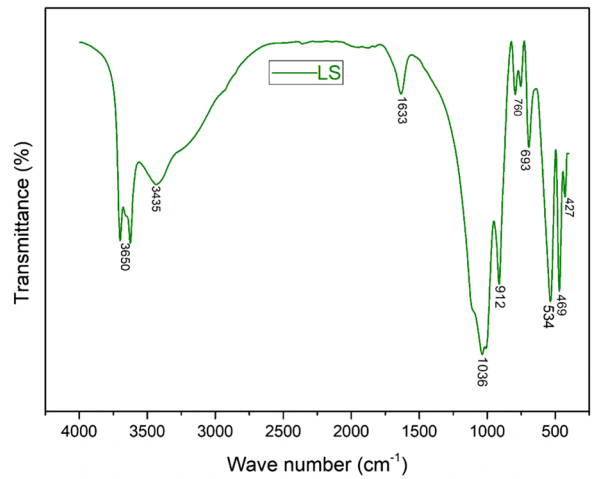

(a) FTIR spectra of lateritic soil (LS).

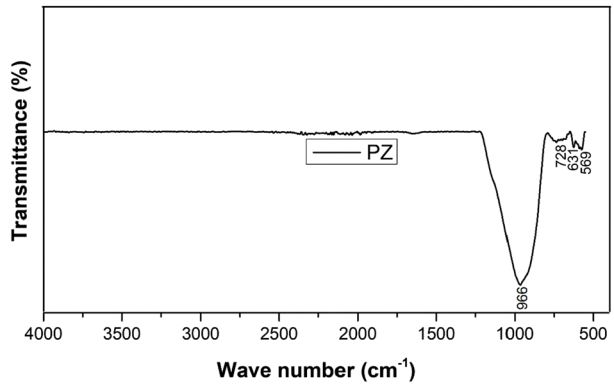

(b) FTIR spectra of natural pozzolan (PZ).

Fig.2 **a** FTIR spectra of lateritic soil (LS). **b** FTIR spectra of natural pozzolan (PZ)

2.3 Experimental Procedures

The particle size distribution of raw materials (laterite soil, natural pozzolan, and sand) was determined according to the standards NF P 18-560 and NF P 94-057 [23].

The plasticity features of the lateritic soil in terms of Atterberg limits were also evaluated according to the NF P94-051 standard [23].

Detailed information regarding the fineness of the aggregates used was recorded by subjecting the materials to the sand equivalent according to the standard NF EN 933-8 [23].

The functional groups within the raw materials and the resulting products were determined with Fourier transform infrared spectroscopy (FTIR) using a Bruker Tensor 37 instrument (Bruker, Germany) with KBr pellets in transmission mode in the range 400–4000 cm^{-1}.

The mineralogical composition of the raw materials and the obtained CEB was analysed with a Bruker D2 Phaser powder X-ray diffractometer (Bruker, Germany), equipped with a flat silicon, low background sample holder, at 30 kV, 10 mA with Cu-Kα radiation ($\lambda = 1.5418$ Å) at a scan speed of 4°/min ranging from 2θ angles of 5 to 70°.

Scanning electron microscopy (SEM) images have been recorded on a JEOL JSM-6510 instrument using a LaB_6 cathode and an acceleration voltage of 20 kV. Before the measurement, samples have been coated with a fine gold layer using a JEOL JFC-1200 Fine Coater. Samples have been mounted on brass sample holders using carbon tape. Energy-dispersive X-ray (EDX) spectra have been recorded using a Bruker XFlash 410-M EDX detector. The signals of carbon, oxygen, gold, zinc and copper are caused by the sample preparation and sample holder. If the sample itself contains one of these elements, it cannot be differentiated

from the "background" intensity. For oxygen, zinc and copper, however, this "background" intensity is comparably low. So, a high EDX percentage of these elements would indicate that they are present in the sample.

Physicochemical performances such as water absorption rate, capillary rise and apparent density were performed as follows. The rate of water penetration by capillary suction into the CEB was measured by sorptivity test following the ASTM C 642. The apparent density was evaluated by hydrostatic measurement according to the standard NF P 98-250-6 [23]. The water absorption test was carried out according to the Cameroonian Standard for CEB [24].

The engineering performances in terms of dry and wet compressive strengths of the produced blocks at 28 days were evaluated according to the Cameroonian Standard 2006 [24].

The fragments from mechanical testing were analysed using optical microscopy (OM) equipped with a stereomicroscope (Ceramics Instruments Model 101 T-MT), a binocular head, and a Table 7 with an integrated camera.

3 Results and Discussion

3.1 Mechanical and Physical Properties of Stabilized CEBs

3.1.1 Visual Appearance

Figure 3 shows the appearance of the samples used for the tests mentioned above. The different bricks stabilized by activation with phosphoric acid solution and hardened at various curing temperatures have a dark brown appearance, while those stabilized by activation with sodium silicate are light brown.

3.1.2 Mechanical Properties of Stabilized CEBs

Dry Compressive Strength Figure 4 depicts the dry compressive strengths of 28-day-old specimens in acidic and

Fig. 3 Appearance of of stabilized CEBs

Table 3 Different proportions of raw materials in the formulation of bricks

Formulation	Lateritic soil (%)	Pozzolan (%)	Sand (%)	Water (g) for CEB^A	Water (g) for CEB^B
$CEB^A{}_X$ and $CEB^B{}_X$	75	15	10	18	16

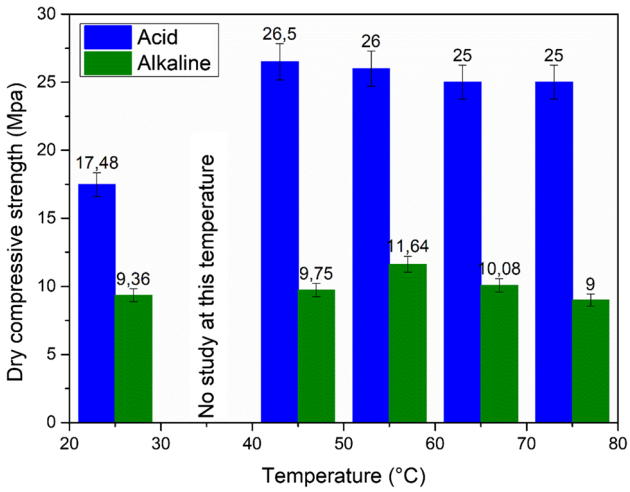

Fig. 4 Dry compressive strength of acid-stabilized CEBs and alkaline-stabilized CEBs cured at different temperatures

alkaline media as a function of curing temperature. The values of dry compressive strength of the sample stabilized by acid activation of pozzolan increase with temperature up to 26.5 MPa at 45° C, then drop to 25 MPa at 75 °C. The dry compressive strength of the sample stabilized by alkaline activation, on the other hand, increases up to 11.64 MPa at 55 °C before dropping to 9 MPa at 75 °C. The dry compressive strength values of CEB stabilized using acid activation were 17.50, 26.50, 26.00, 25.00 and 25 MPa for 25, 45, 55, 65, and 75° C, respectively. Those stabilized with alkaline-based binder were 9.36, 9.75, 11.64, 10.08, 9.36 MPa for 25, 45, 55, 65, and 75 °C, respectively.

Initially, it is noted that the rise of temperature increases the compressive strength of CEBs in both cases of stabilization. However, the stabilization is more significant in an acidic medium resulting in better strength development. These results show the temperature is indeed a kinetic factor for the stabilization of bricks by the activated geopolymer binder in both acid and alkaline media. The increase in temperature promotes the dissolution of the amorphous aluminosilicate phase as well as the polymerization/polycondensation are the geopolymeric poly-siliate-ferro-siloxo (N–A–S–H) and poly-phospho-sialate-siloxo (P–A–S–H) networks in alkaline and acidic media, respectively [3, 25]. The high compressive strength values of the products obtained in an acidic medium depict that the polycondensation/polymerization emerges more in an acidic medium and that the P–A–S–H chain is stronger than N–A–S–H. The decrease in compressive strength is probably because above 45 °C (in acidic medium) and 55 °C (in alkaline medium), the amount of water present is no longer sufficient for the efficient geopolymerization as there is probably leaching of the water which causes micro-cracking which is also detrimental to the mechanical properties [26]. For volcanic ash-based geopolymer binders, these phenomena are often observed above 70 °C [27], and the contrary observed in this work is probably due to the presence of hygroscopic species such as clay minerals in the matrix where geopolymerization takes place.

Wet Compressive Strength The images shown in Fig. 5a are CEB stabilized by acid activation and alkaline activation of natural pozzolan after 24 h in water. All the bricks cured at the different study temperatures show good resistance in water after 24 h. However, the water in which the alkali-stabilized bricks (series B) are immersed turns yellow after 24 h. This coloration is due to the fine particles of the lateritic soil leached by the water, which is an aggressive agent [13].

Figure 5b depicts the temperature-dependent evolution of the wet compressive strength of the 28-day-old CEB samples. It can be seen that wet compressive strength evolution shows a similar trend as the dry compressive strength. Furthermore, the wet compressive strengths obtained at 45 and 55 °C (9.75 and 5.50 MPa) for CEB activated in acid and alkaline media, respectively, are significantly higher than those obtained at ambient temperature. In the case of acid stabilization, CEB cured at room temperature lose 50% of their strength after 24 h in the water, while those stabilized at 45 °C and above lose about 60% of their strength. However, in the case of CEB stabilized by alkaline activation, CEB cured at room temperature lose 65% of their strength, while those cured at 45, 55, 65, and 75 °C lose about 55% of their dry strength. This observation shows that the increase in curing temperature is more favourable for the stabilization of CEB by alkaline activation of natural pozzolan because those stabilized by acid activation and cured at room temperature have good water resistance. In fact, these losses in strength are attributed to the weakening of the geopolymer network that provides the link between the unreacted particles due to its hydrolysis or hydration, forming the silanol Si–OH and aluminol Al–OH bonds weakening the geopolymer network [16, 28].

In general, there is a great advantage in using oven curing to improve the mechanical properties of CEBs stabilized with geopolymer binder when in contact with water [29].

3.1.3 Physicochemical Properties of Stabilized CEBs

Bulk Density by Hydrostatic Measurement Figure 6 shows the dry and wet bulk density of acid-stabilized and alkaline-stabilized CEBs as a function of the curing temperature. For acid-stabilized CEBs, the dry bulk density is 1.73, 1.88, 1.85, 1.74, and 1.72 g/cm^3 and the wet bulk density is 1.81, 1.97, 1.93, 1.80, and 1.76 g/cm^3 for room temperature, 45 °C, 55 °C, 65 °C, and 75 °C respectively. Concerning the alkali-stabilized CEBs, the dry bulk density is 1.56, 1.64, 1.71, 1.61, and 1.61 g/cm^3 and the wet bulk density is 1.63, 1.69, 1.76, 1.65, and 1.65 g/cm^3 for room temperature, 45 °C, 55 °C,

Fig. 5 **a** Water resistance of stabilized CEB. **b** Wet compressive strength of acid-stabilized CEBs and alkaline-stabilized CEBs cured at different temperatures

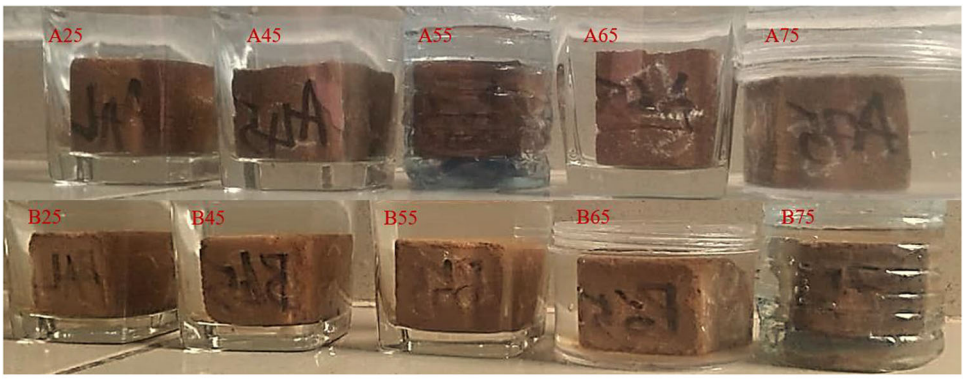

(a) Water resistance of stabilized CEB.

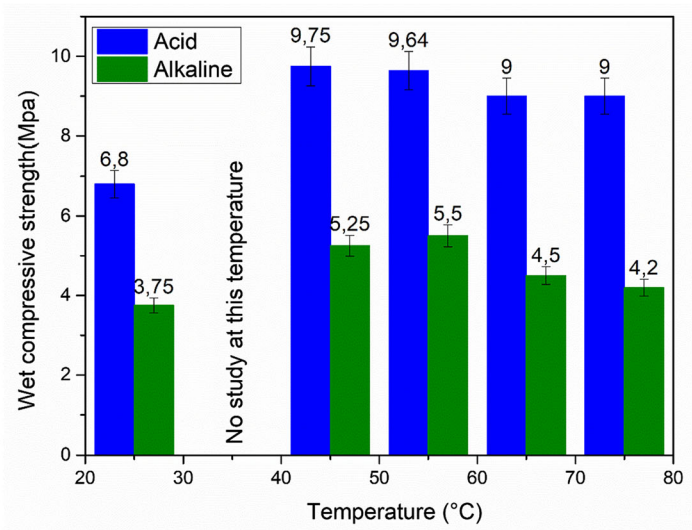

(b) Wet compressive strength of acid-stabilized CEBs and alkaline-stabilized CEBs cured at different temperatures.

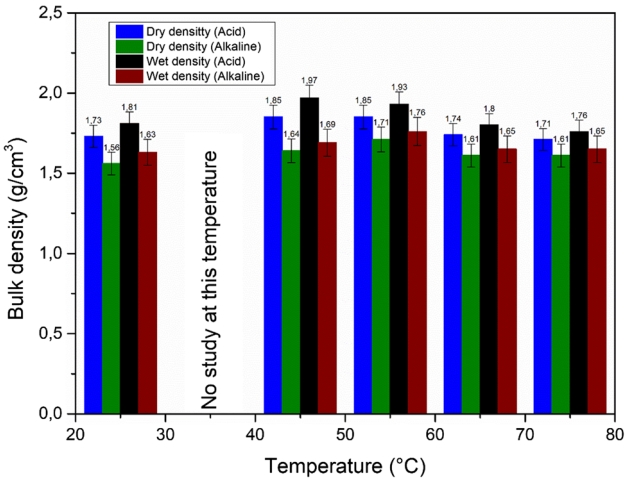

Fig. 6 Bulk density of CEBs acid and alkaline cured at different temperatures

65 °C, and 75 °C, respectively. It can be seen that for CEB stabilized by acid activation, the bulk densities increased up to 1.85 g/cm^3 (dry density) and 1.97 g/cm^3 (wet density) at 45 °C and then decrease beyond this temperature. In contrast, for those stabilized by alkaline activation, these densities increased up to 1.71 g/cm^3 (dry density) and 1.76 g/cm^3 (wet density) at 55 °C and then decrease beyond this temperature. This variation of the densities with the curing temperature is consistent with the compressive strength results discussed previously, as materials at this temperature have the highest compressive strengths. This is justified by the fact that these temperatures were favourable for the acceleration of the geopolymerization kinetics leading to a significant dissolution of the silica and alumina of the aluminosilicate source and a better polycondensation which would increase the densification of the materials and their mechanical resistance [27]. The improvement of these densities at these polymerization temperatures, namely 45 and 55 °C, is justified by the

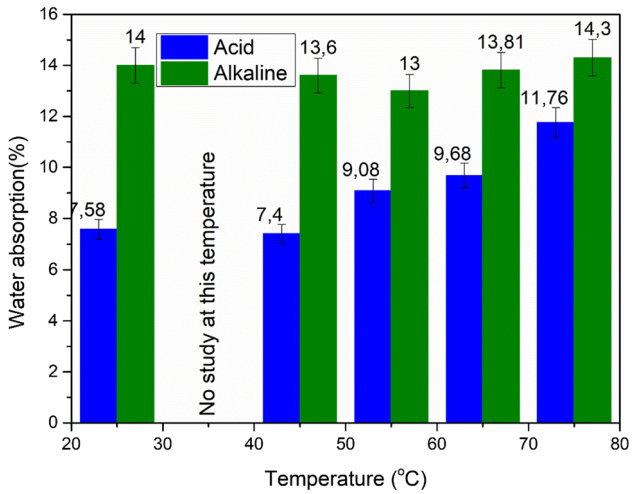

Fig. 7 Water absorption of CEBs acid and alkaline cured at different temperatures

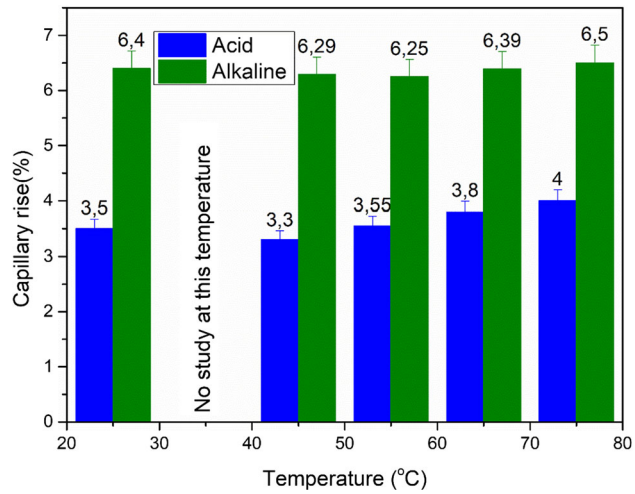

Fig. 8 Capillary rise of 28-day-old CEBs acid and alkaline cured at different temperatures

fact that 45 and 55 °C are adequate to cause residual dehydration capable of amplifying the pores in the materials [30]. It is significant to note that all the densities obtained by acid activation are within the limit required by the Cameroonian standard for construction (1.7 to 2 g/cm^3) [28]. However, in an alkaline environment, only CEB at 55 °C has a density within this acceptable range. This observation confirms once again that pozzolan is more reactive in an acidic medium than in an alkaline medium.

3.3.1.2.2. Water Absorption

Figure 7 shows the water absorption percentage of CEBs as a function of the curing temperature. In the acidic environment, these values are 7.58, 7.40, 9.08, 9.68 and 11.76% for 25, 45, 55, 65, and 75 °C, respectively. In alkaline media, it was 14.00, 13.60, 13.00, 13.81, and 14.30% for 25, 45, 55, 65, and 75 °C, respectively. These results show that in an acidic activation, the water absorption rate of CEB decreases until 45 °C and then increases beyond this temperature. As described above (Sect. 3.1.1.2), the increment in temperature above 45 °C leads to the formation of large pores and cracks that allow water to pass through. In an alkaline activation, on the other hand, the lowest water absorption rate of 13% is still observed at 55 °C. At this temperature, the material had the best mechanical strength. Therefore, it can be said that the water absorption rate evolves inversely to the compressive strength, although the CEBs stabilized by acid activation have the lowest water absorption percentage values. In general, the increase in these water absorption rates after 45 and 55 °C would be explained by the fact that at these temperatures, the geopolymer consolidation reactions would be more important, leading to a reduction in the porosity [31]. In addition, all samples have values of percentage of water absorption which respect the value required by the ASTM standard for construction materials which requires a percentage of water absorption below or equal to 15% [32, 32].

3.3.1.2.3. Capillary Rise

The results of the capillary rise of CEBs stabilized by acid activation on the one hand and by alkaline activation on the other as a function of curing temperature are shown in Fig. 8. This test lasted one hour and was performed continuously. At room temperature (25 °C), 45, 55, 65, and 75 °C, the capillary rise values of the CEB stabilized by acid activation are 3.50, 3.30, 3.55, 3.80, and 4.00%, respectively. For those made with alkali-activated binder, the values were 6.40, 6.25, 6.39, 6.41, and 6.50% at room temperature (25 °C), 45, 55, 65, and 75 °C, respectively. It is worth noting that the lowest values of capillary rise were obtained at 45 °C in acid medium and at 55 °C in alkaline medium. These values are 3.30 and 6.25% at 45 °C in acid medium and at 55 °C in alkaline medium, respectively. This observation is consistent with the behaviour of the bulk density and water absorption rate of the stabilized CEB in acidic medium. In fact, above those temperatures (45 and 55 °C), there is significant leaching of water, which creates the pores [33]. These pores will allow more water to pass through, increasing the sample's water permeability.

Conclusively, the produced CEBs present the lowest capillary rise values between 45 and 55 °C, corresponding to the range of the best compressive strengths. CEB stabilized by alkaline activation seems more permeable than those stabilized by acid activation.

3.1.4 Microstructural properties of CEBs

3.3.1.2.4. PXRD

Figure 9 a-b shows the diffractograms of selected CEBs stabilized by acid activation and alkaline activation of natural

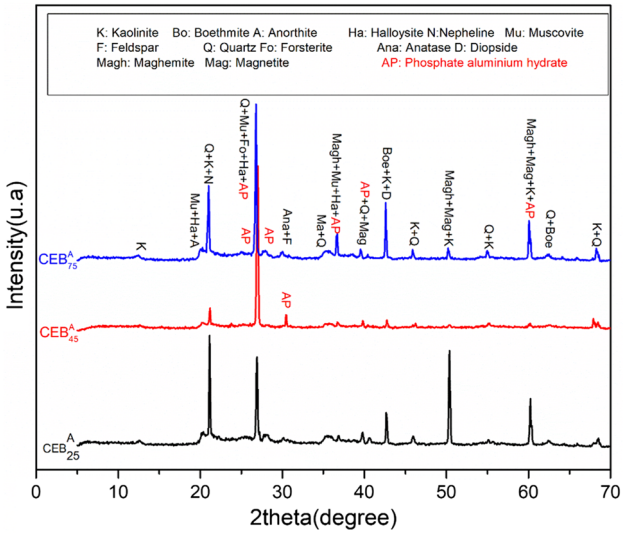

(a) XRD of 28 days old CEBs acid cured at different temperatures.

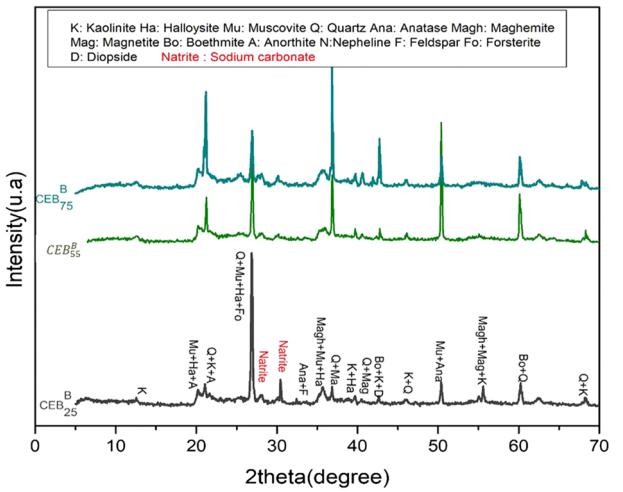

(b) XRD of 28 days old CEBs alkaline cured at different temperatures.

Fig. 9 **a** XRD of 28-day-old CEBs acid cured at different temperatures. **b** XRD of 28-day-old CEBs alkaline cured at different temperatures

pozzolan with different curing temperatures (room temperature, 45 and 75 °C in acid medium and room temperature, 55 and 75 °C in alkaline medium).

From Fig. 9a, the 28-day-old CEBs, stabilized using an acid activation binder, mainly contain quartz, halloysite, anatase, muscovite, forsterite, and diopside. These originated from the feedstock, i.e. lateritic soil and natural pozzolan (Fig. 1b). However, the intensity of the peaks seem to be influenced by the curing temperature. At 45 °C in an acid medium, there is a significant reduction in the peak intensity of kaolinite, magnetite, maghemite, and nepheline. This may be due to a significant dissolution of these phases by the phosphoric acid solution, which improved the geopolymer network and their mechanical strength. Furthermore, the formation of hydrated phosphate aluminate and iron aluminium phosphate oxide is noted [2] as well as the presence of an increased background between 20 and 35° (2θ) characteristic of the amorphous phases due to the newly formed geopolymer phase after phosphoric acid activation [34]. The improved physicochemical and mechanical properties obtained previously at 45 °C are due because both the amorphous and crystalline phases participate in the geopolymerization reaction at this temperature.

Similarly, crystalline phases were identified in the diffractograms of the CEB stabilized by alkaline activation of natural pozzolan (Fig. 9b). Here, the low decrease in the central peak located in the amorphous zone (at ~ 25 °) also reflects the weak dissolution of aluminosilicate phases in alkaline medium. The decrease emerges with increasing temperature. The existence of dump between 20 and 35 °(2θ) on these diffractograms shows once again the formation of amorphous phase which mainly comes from the transformation of amorphous aluminosilicate phases contained in the natural pozzolan into geopolymer binder which is also amorphous phases. This dump increases with increasing curing temperature. It is also noticeable the quasi-disappearance of sodium carbonate peaks from the carbonation reaction between free Na^{+} and atmospheric CO_2 at 55 and 75 °C. This fact was also observed by Sore et al., 2017 during the stabilization of CEB by metakaolin-based alkaline geopolymer binder [5].

The coexistence of crystalline and geopolymer networks in both environments is beneficial for the mechanical properties of the obtained products because these minerals play the role of aggregates even at the microscopic scale [35].

3.3.1.2.5. FTIR

Figure 10a, b depicts the infrared spectra of samples stabilized by acid activation and alkaline activation at various curing temperatures (room temperature, 45 °C and 75 °C in acid medium and room temperature, 55 °C and 75 °C in alkaline medium). Four spectral regions can be noticed, similar to the spectrum of LS (Fig. 2), with minor modifications. In general, after the activation of precursor materials for geopolymerization, the shift of the main band of the aluminosilicate phases contained in this material located at around 1000 cm^{-1} is observed [3, 16]. This shift reflects a restructuring of the aluminosilicate phases after the polymerization/polycondensation reaction. The absence of this phenomenon is due to the predominance of the crystalline aluminosilicate phases over the amorphous ones. This observation once again reflects the low dissolution of aluminosilicates present in the lateritic soil in both activation media. The O–H stretching vibrations of the inner surface of hydroxyl groups of hydroxylated minerals, characteristic of the presence of residual kaolin and halloysite, are attributed to the absorption bands around 3670 cm^{-1} for all CEB [36]. The presence of bands around 790, 693, and 536 cm^{-1} in both

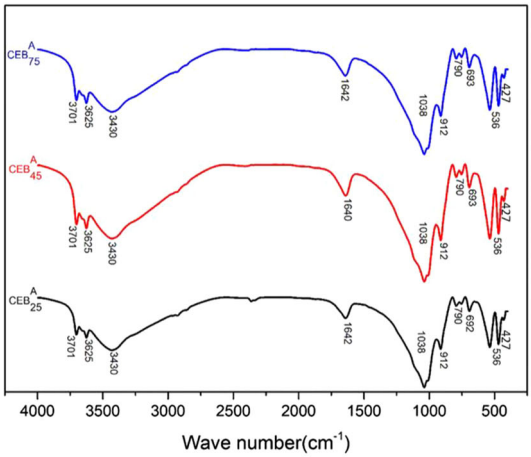

(a) FTIR spectra of 28 days old CEBs acid cured at different temperatures.

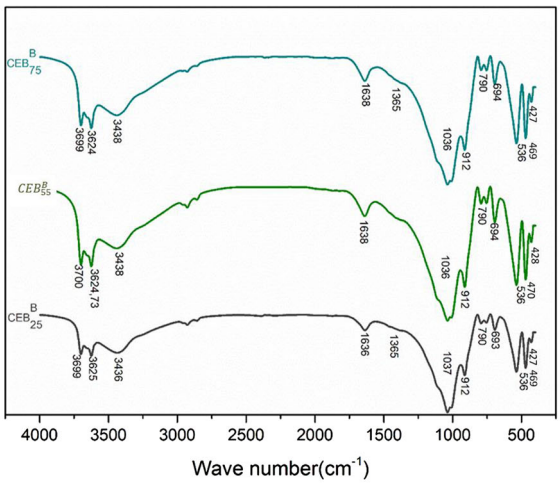

(b) FTIR spectra of 28 days old CEBs alkaline cured at different temperatures.

Fig. 10 **a** FTIR spectra of 28-day-old CEBs acid cured at different temperatures. **b** FTIR spectra of 28-day-old CEBs alkaline cured at different temperatures

stabilization cases corresponds to the Si–O–Si, Fe–O–Fe, Si–O–Al, and Fe–O–Si bands observed during the reaction [16, 37]. In the specific case of stabilization by alkaline activation, the band around 1365 cm^{-1} corresponds to C-O bond elongation vibrations in sodium carbonate [5]. This band seems to disappear with the increase in curing temperature.

3.3.1.2.6. Optical Microscopic (OM) and Scanning Electron Microscopy/Energy-Dispersive X-ray Spectroscopy (SEM/EDX)

Figures 11, 12, 13 and 14 show optical micrographs and scanning electron micrographs of CEB stabilized by acid activation and alkaline activation at various curing temperatures. In the view of the different micrographs, only the sample cured at 45 °C in an acid medium and those cured at 55 °C in an alkaline medium are homogeneous. This homogeneity could be related to the formation of a greater binder phase, ensuring better cohesion between different components within the matrices. The results are consistent with the findings of the PXRD (Sect. 3.1.3.1). At room temperature (CEB^A_{25} and CEB^B_{25}), the alkaline activation products contain more macrospores and more undissolved particles than the acid activation products. Although room temperature slows down the geopolymerization process, this could be justified by the aforementioned great dissolution of pozzolan in acidic environments. The presence of macropores in some materials confirms thus the above-mentioned significant water permeability capacity of these materials. The observed white deposits could be caused by the fact that after 28 days of exposure to room temperature, the free Na^+ ions in the matrices reacted with the carbon dioxide in the air, resulting in the appearance of efflorescence [38, 39]. This is consistent with the FTIR results (Sect. 3.1.3.2), which revealed the appearance of a band around 1365 cm^{-1}, which is typical of C-O type bonds.

At 45 and 55 °C, the compact and homogeneous micrographs of the acid-activated and alkaline-activated stabilized CEBs, respectively (CEB^A_{45} and CEB^B_{55}), corroborate with the best physicochemical and mechanical properties obtained at this temperature. This observation suggests that this temperature is suitable for significant aluminosilicate dilution, favouring the formation of a significant amount of amorphous geopolymer phase [40]. However, the micrographs of the products obtained at 75 °C (CEB^A_{75} and CEB^B_{75}) are compact but show cracks and deterioration. This explains the decrease in compressive strength at this temperature. This finding supports the hypothesis that while the temperature is an essential factor in improving the performance of geopolymers, high temperatures can cause material deterioration, resulting in lower performance.

Figures 13 and 14 and Table 4 present the EDX analysis of the selected matrices cured at 25, 45, and 75 °C in an acid medium and at 25, 55, and 75 °C in an alkaline medium. From Fig. 13, the presence of O, Si, Al, Fe and P elements confirmed the formation of the phosphate binder of the ferro-silico-aluminophosphate type within the matrices (P–A(F)–S–H) [2]. This means the formation of the P–A(Fe) –S–H geopolymer binder type during the stabilization process. It is worth noting that the curing temperature is beneficial for producing sufficient phosphoric binder. Thus at 25 °C, the semi-quantitative chemical composition was 36 wt% of O, 14 wt% of Si, 10 wt% of Al, 5 wt% of Fe and 3 wt% of P. With increasing curing temperatures up to 75 °C, the EDX analysis (Table 4) highlighted at 45 °C 37 wt% de O, 20 wt% de Si, 9 wt% de Al, 7 wt% de Fe and 3 wt% de P and at 75 °C 41 wt% of O, 22 wt% of Si, 10 wt% of Al, 4 wt% of Fe, and 4 wt% of P.

From the block stabilized using the alkaline solution, regardless of the range of the curing temperatures, all the data indicated that O, Si, Al, Fe, and Na remained dominant

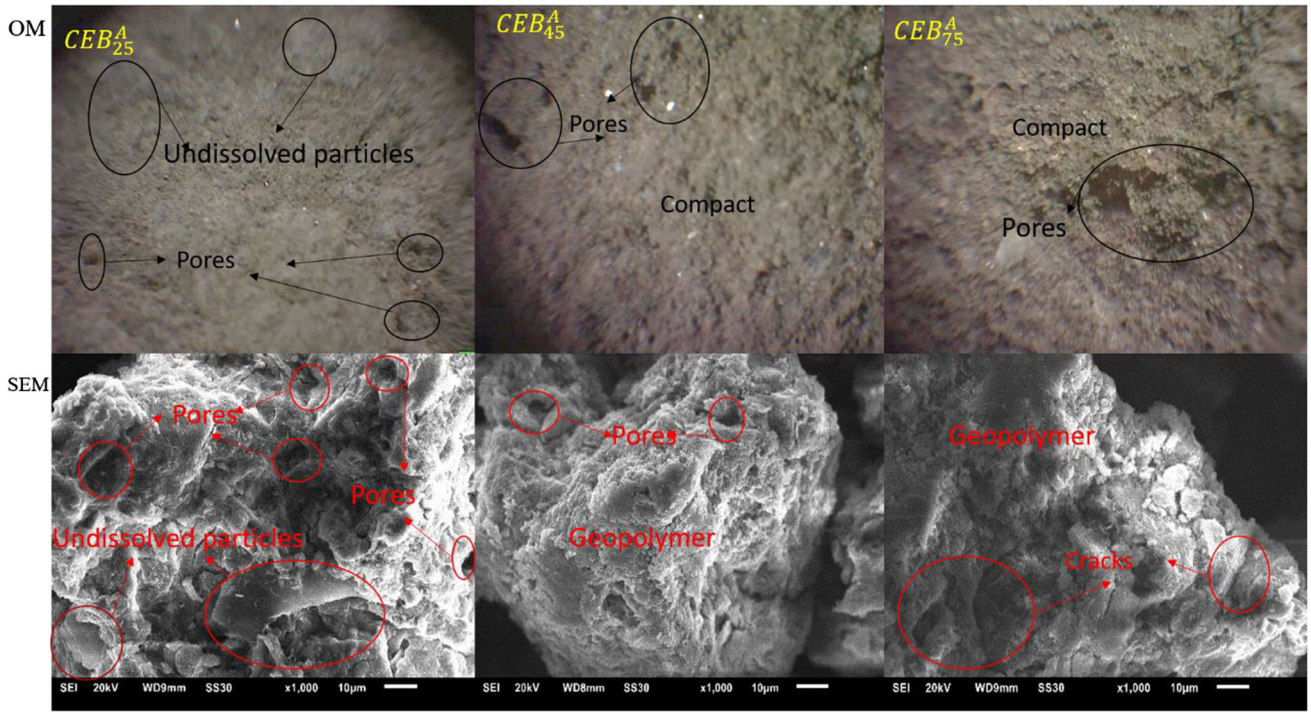

Fig. 11 Optical (upper row) and scanning electron (lower row) micrographs of 28-day-old CEBs acid cured at different temperatures

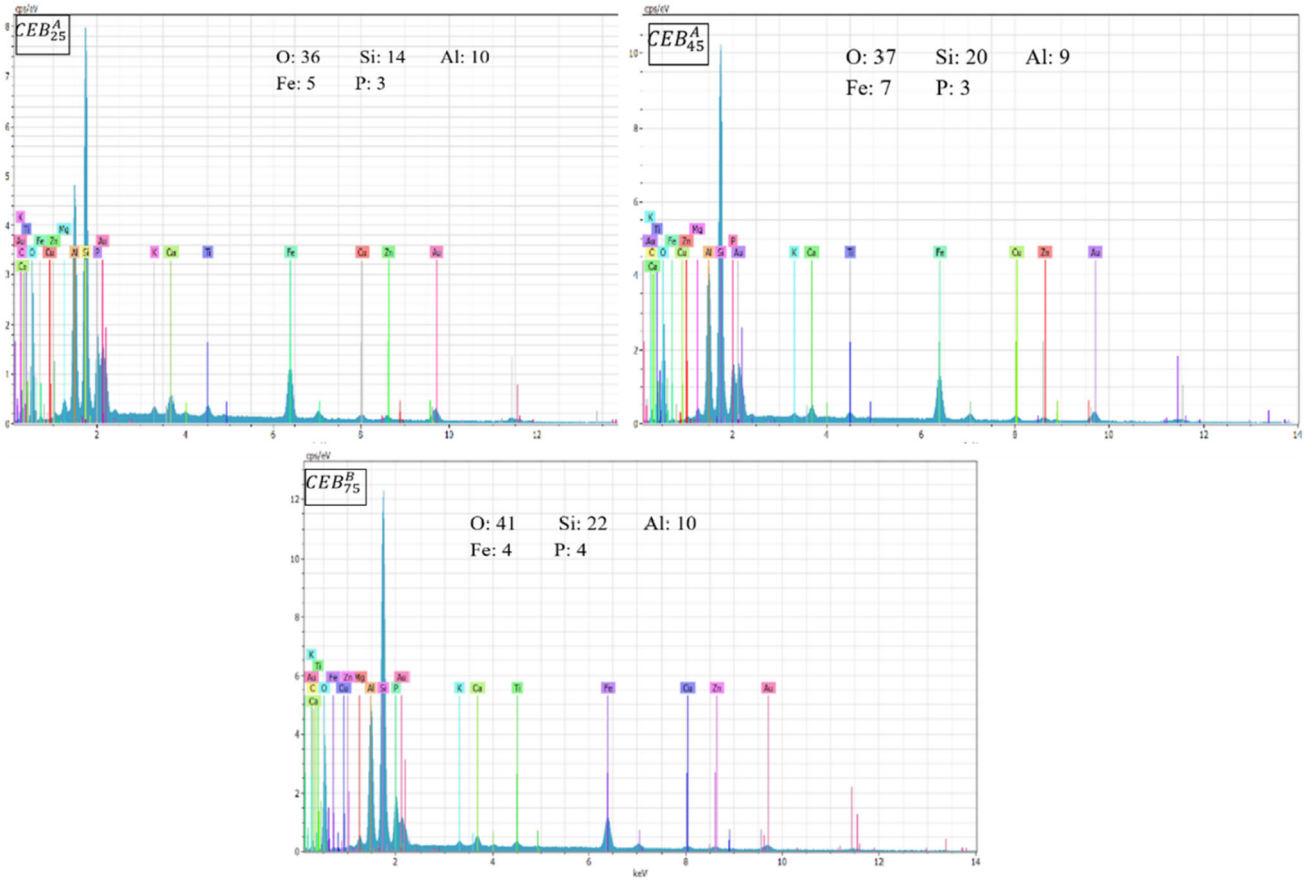

Fig. 12 EDX analysis of 28-day-old CEBs acid cured at different temperatures

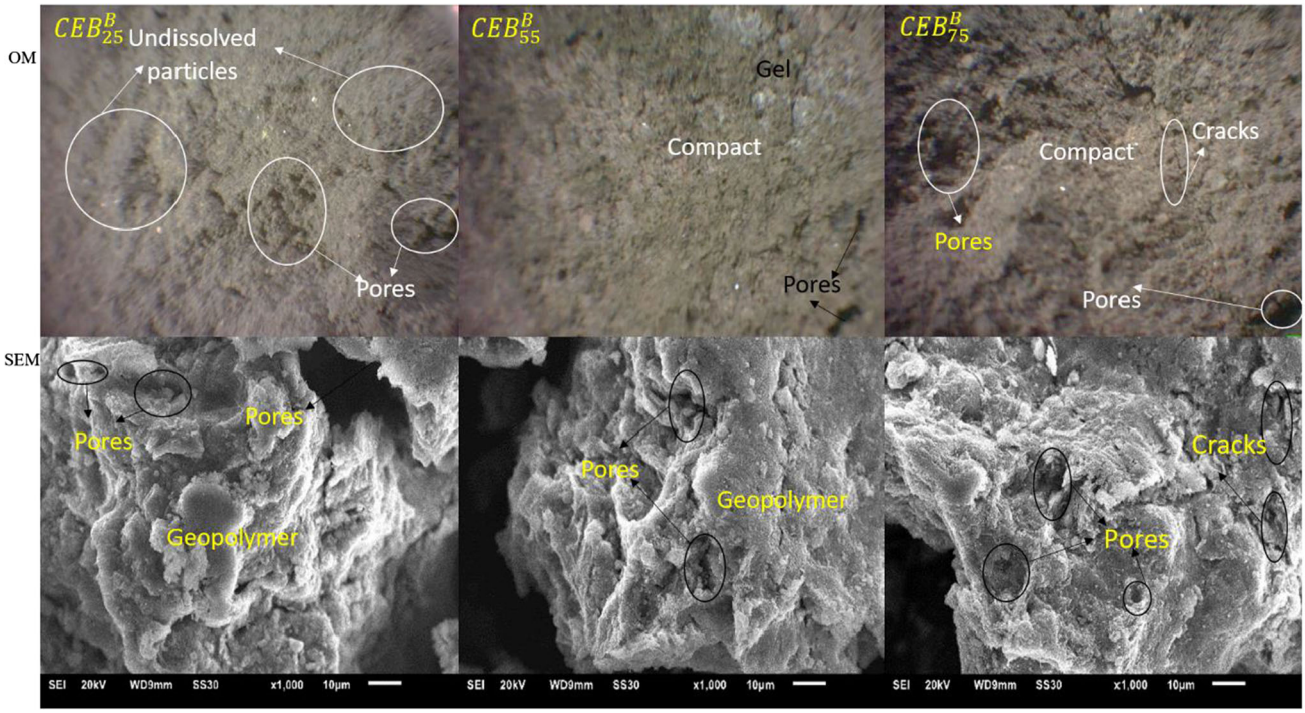

Fig. 13 Micrograph of 28-day-old CEBs alkaline cured at different temperatures

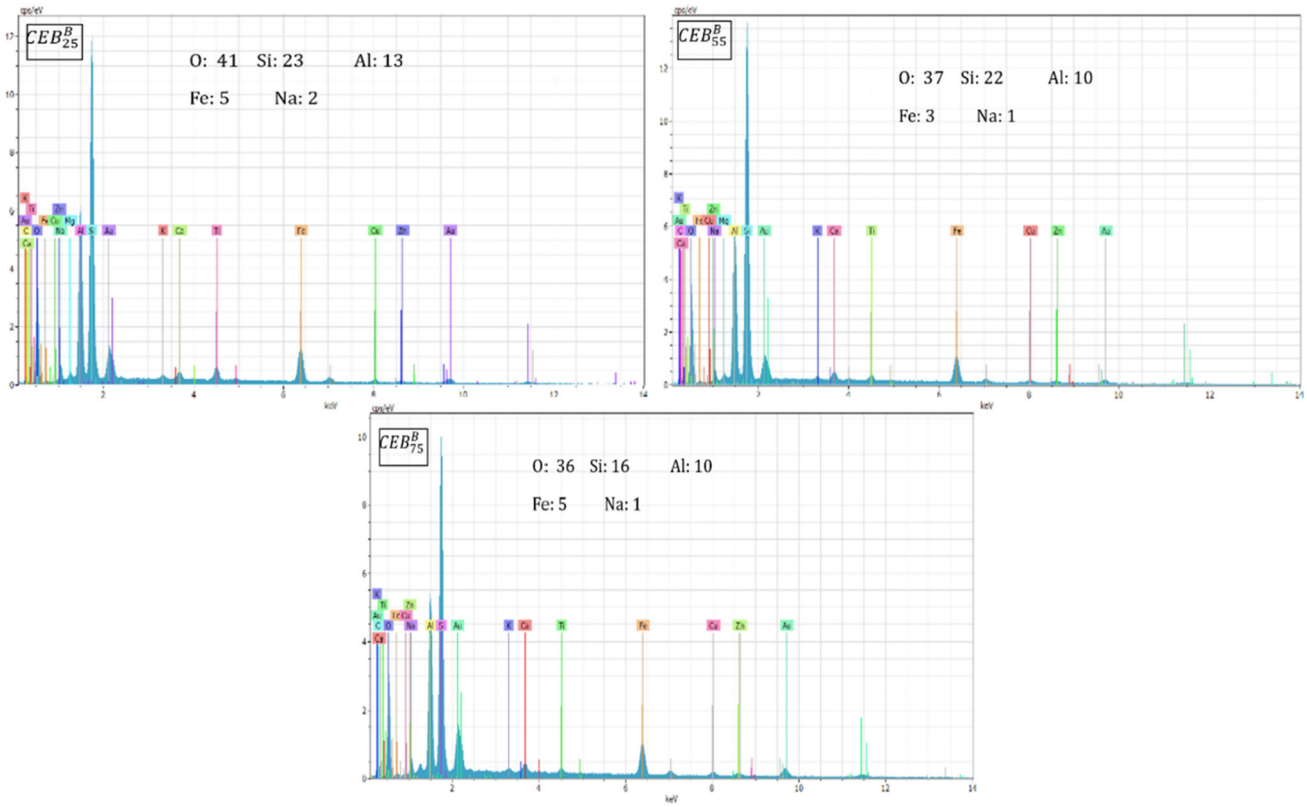

Fig. 14 EDX analysis of 28-day-old CEBs alkaline cured at different temperatures

Table 4 EDX analysis of laterite brick stabilized by acid and alkali activation of pozzolan

Acid activation			
Chemical composition	CEB^{A}_{25}	CEB^{A}_{45}	CEB^{A}_{75}
O	36	37	41
Si	14	20	22
Al	10	9	10
Fe	5	7	4
P	3	3	4
Si/Al	1.40	2.22	2.20
Si/Fe	2.80	2.86	5.50
Si/P	4.67	6.67	5.50
Al/P	3.33	3.00	2.50
Alkaline activation			
Chemical composition	CEB^{B}_{25}	CEB^{B}_{55}	CEB^{B}_{75}
O	41	37	36
Si	23	22	16
Al	13	10	10
Fe	5	3	5
Na	2	1	1
Si/Al	1.77	2.20	1.60
Si/Fe	4.60	7.33	3.20
Si/Na	11.50	22	16
Al/Na	6.5	10	10

elements within the matrices. This means the formation of the N–A(Fe) –S–H geopolymer binder type during the stabilization process [41]. At room temperature, the recorded data are 41 wt% of O, 23 wt% of Si, 13 wt% of Al, 5 wt% of Fe, and 2 wt% of Na. These data correspond to 37 wt% de O, 22 wt% de Si, 10 wt% de Al, 3 wt% de Fe and 1 wt% of Na at 55 °C and to 36 wt% de O, 16 wt% de Si, 10 wt% de Al, 5 wt% de Fe and 1 wt% of Na at 75 °C.

Moreover, the analysis of the Si/Al ratio (Table 4) shows that the highest values of this ratio are obtained at 45 and 55 °C, respectively, in acid and alkaline media. These temperatures are those at which the products presented the best physical–mechanical proprieties. These results corroborate the results of the XDR analysis which showed a better dissolution of the reactive phase at these temperatures.

4 Conclusion

The purpose of this work was to investigate the effect of curing temperature on CEB-based lateritic soil stabilized by pozzolan-based acid-activated and alkali-activated geopolymer binders. It also aimed to determine the optimal curing temperature for the production of stabilized bricks. The different results obtained revealed that:

- The dry compressive strength of the acid-stabilized specimen increases with temperature up to 45 °C and then drops to 75 °C, whereas the alkali-stabilized specimen increases with temperature up to 55 °C and then drops to 75 °C.
- The CEBs have the lowest capillary rise values at 45 and 55 °C, the temperatures at which CEBs have the highest compressive strengths.
- At 45 and 55 °C, the CEB stabilized by acid and alkaline activation (CEB^{A}_{45} and CEB^{B}_{55}), respectively, exhibits compact microstructure, which correlates with the improved physical–mechanical properties obtained at this temperature.

According to these aforementioned results, the curing temperature appears as a significant parameter during the stabilization of lateritic soil based on the natural pozzolan-based acid and alkaline geopolymer binders. However, temperatures above 45 °C for acid medium and 55 °C for alkaline medium are detrimental for the mechanical performance of geopolymer products.

Acknowledgements The authors thank LABOGENIE and ENSET (Douala-Cameroon) for extending all the facilities to carry out this research.

Author Contributions RATK, M-AE, and ST involved in validation, methodology, writing—review and editing, visualization, and original draft. RATK, LT, ST, IE, and JC involved in conceptualization, methodology, investigation, and writing—original draft. RATK, TL, AS, BT, and DW involved in PXRD, SEM/EDS and FTIR analysis, validation, writing—review and editing, and visualization. ST, LT, and JDN involved in methodology, writing review and editing, original draft, supervision, methodology, and resources. CJ and M-AE involved in resources and supervision.

Funding The authors of manuscript did not receive any funding and grants for this work.

Data Availability All data generated or analysed during this study are included in this article.

Declarations

Conflict of interest The authors declare that they have no conflict of interest.

Consent to Participate Not applicable.

Consent for Publication Not applicable.

References

1. Djobo, J.N.Y.; Tchadjié, L.N.; Tchakoute, H.K.; Kenne, B.B.D.; Elimbi, A.; Njopwouo, D.: Synthesis of geopolymer composites from a mixture of volcanic scoria and metakaolin. Integr. Med. Res. (2014). https://doi.org/10.1016/j.jascer.2014.08.003
2. Mimboe, A.G.; Abo, M.T.; Djobo, J.N.Y.; Tome, S.; Kaze, R.C.; Deutou, J.G.N.: Lateritic soil based-compressed earth bricks stabilized with phosphate binder. J. Build. Eng. **31**, 101465 (2020). https://doi.org/10.1016/j.jobe.2020.101465
3. Tome, S.; Etoh, M.A.; Etame, J.; Kumar, S.: Improved reactivity of volcanic ash using municipal solid incinerator fly ash for alkali-activated cement synthesis. Waste Biomass Valoriz. **11**, 3035–3044 (2020). https://doi.org/10.1007/S12649-019-00604-1
4. Rodrigue, C.; Tome, S.; Lecomte-nana, G.L.; Adesina, A.; Essaedi, H.; Kumar, S.; Alomayri, T.; Kamseu, E.; Chinje, U.: Materialia Development of alkali-activated composites from calcined iron-rich laterite soil. Materialia **15**, 101032 (2021). https://doi.org/10.1016/j.mtla.2021.101032
5. Ntimugura, F.; Sore, S.O.; Bello, L.; Messan, A.: The Influence of Metakaolin from Saaba (Burkina Faso) over physico-mechanical and durability properties of mortars, open. J. Civ. Eng. **07**, 389–408 (2017). https://doi.org/10.4236/ojce.2017.73027
6. Bergamonti, L.; Taurino, R.; Cattani, L.; Ferretti, D.; Bondioli, F.: Lightweight hybrid organic–inorganic geopolymers obtained using polyurethane waste. Constr. Build. Mater. **185**, 285–292 (2018)
7. Tchadjie, L.N.; Ekolu, S.O.: Enhancing the reactivity of aluminosilicate materials toward geopolymer synthesis. J. Mater. Sci. **53**, 4709–4733 (2018). https://doi.org/10.1007/s10853-017-1907-7
8. Djobo, J.N.Y.: Effets de l'incorporation d'adjuvants minéraux sur les propriétés de ciments géopolymères à base de scories volcaniques, (2013)
9. Tchakoute, H.K.; Elimbi, A.; Yanne, E.; Djangang, C.N.: Utilization of volcanic ashes for the production of geopolymers cured at ambient temperature. Cem. Concr. Compos. **38**, 75–81 (2013). https://doi.org/10.1016/j.cemconcomp.2013.03.010
10. Kamwa, T.; Aurelie, R.; Tome, S.; Judicaël, C.; Spieß, A.; Fetzer, M.N.A.; Kamseu, E.; Janiak, C.: Stabilization of Compressed Earth Blocks (CEB) by pozzolana based phosphate geopolymer: Physico-mechanical, structural and microstructural investigations, (n.d.) 1–22
11. Wang, W.; Gan, Y.; Kang, X.: Synthesis and characterization of sustainable eco-friendly unburned bricks from slate tailings. J. Mater. Res. Technol. **14**, 1697–1708 (2021). https://doi.org/10.1016/j.jmrt.2021.07.071
12. Diaz, E.I.; Allouche, E.N.; Eklund, S.: Factors affecting the suitability of fly ash as source material for geopolymers. Fuel **89**, 992–996 (2010). https://doi.org/10.1016/j.fuel.2009.09.012
13. Aurelie, R.; Kamwa, T.; Tome, S.; Chongouang, J.; Eguekeng, I.; Spieß, A.; Fetzer, M.N.A.; Elie, K.; Janiak, C.; Etoh, M.: Stabilization of compressed earth blocks (CEB) by pozzolana based phosphate geopolymer binder: physico-mechanical and microstructural investigations. Clean. Mater. **4**, 100062 (2022). https://doi.org/10.1016/j.clema.2022.100062
14. Idriss, E.; Tome, S.; Kamwa, T.; Aurelie, R.; Nana, A.; Deutou, J.G.; Chongouang, N.; Alex, J.; Markus, S.; Christoph, N.A.F.; Etoh, M.A.: Engineering and structural properties of compressed earth blocks (CEB) stabilized with a calcined clay-based alkali-activated binder. Innov. Infrastruct. Solut. (2022). https://doi.org/10.1007/s41062-022-00760-9
15. Messaoudene, I.; Molez, L.; Amriou, A.: Effet du Sable de dune sur la Durabilité du Béton de Terre Stabilisée et Compressée. Ajce. **38**, 101–104 (2020)
16. Rodrigue, C.; Venyite, P.; Nana, A.; Nemaleu, D.; Kouamo, H.; Rahier, H.; Kamseu, E.; Chinje, U.; Leonelli, C.: Meta-halloysite to improve compactness in iron-rich laterite-based alkali activated materials. Mater. Chem. Phys. **239**, 122268 (2020). https://doi.org/10.1016/j.matchemphys.2019.122268
17. Lu, Y.; Wang, R.; Lu, X.; Li, J.; Wang, T.: Reprint of Genesis of halloysite from the weathering of muscovite: Insights from microscopic observations of a weathered granite in the Gaoling Area, Jingdezhen, China. Appl. Clay Sci. (2015). https://doi.org/10.1016/j.clay.2015.08.024
18. Liew, Y.M.; Heah, C.Y.; Mohd Mustafa, A.B.; Kamarudin, H.: Structure and properties of clay-based geopolymer cements: a review. Prog. Mater. Sci. **83**, 595–629 (2016). https://doi.org/10.1016/j.pmatsci.2016.08.002
19. Kabre, S.; Ouedraogo, F.; Naon, B.; Messan, A.: Évaluation des propriétés thermo-hydro-mécaniques des briques en terre compressée (BTC) issues de la carrière de Matourkou, au Burkina Faso Résumé. Afr. Sci. **15**, 12–22 (2019)
20. Criado, M.; Fernández-Jiménez, A.; Palomo, A.; Sobrados, I.; Sanz, J.: Effect of the SiO_2/Na_2O ratio on the alkali activation of fly ash. Part II:29Si MAS-NMR Survey. Microporous Mesoporous Mater. **109**, 525–534 (2008). https://doi.org/10.1016/j.micromeso.2007.05.062
21. Kriskova, L.; Machiels, L.; Pontikes, Y.: Inorganic polymers from a plasma convertor slag: effect of activating solution on microstructure and properties. J. Sustain. Metall. **1**, 240–251 (2015). https://doi.org/10.1007/s40831-015-0022-8
22. Tchakoute, H.K.; Rüscher, C.H.; Djobo, J.N.Y.; Kenne, B.B.D.; Njopwouo, D.: Influence of gibbsite and quartz in kaolin on the properties of metakaolin-based geopolymer cements. Appl. Clay Sci. (2015). https://doi.org/10.1016/j.clay.2015.01.023
23. NF-P-98-086-2011-Dimensionnement-structurel-des-chaussées-routières.pdf, (n.d.).
24. Camerounaise, N.; Ii, C.: CHAPITRE I: Quelques generalité sur les briques et la science géopolymère, (n.d.)
25. Criado, M.; Aperador, W.; Sobrados, I.: Microstructural and mechanical properties of alkali activated Colombian raw materials. Materials (Basel) **9**, 158 (2016). https://doi.org/10.3390/ma9030158
26. Tchadjié, L.N.; Ekolu, S.O.: Effect of bauxite content and fineness on compressive strength of volcanic ash-based geopolylmer mortars, pp. 0–5 (2018)
27. Djobo, J.N.Y.; Kumar, S.; Elimbi, A.: Reactivity of volcanic ash in alkaline medium, microstructural and strength characteristics of resulting geopolymers under different synthesis conditions. J. Mater. Sci. **51**, 10301–10317 (2016). https://doi.org/10.1007/s10853-016-0257-1
28. Lemougna, P.N.; Melo, U.F.C.; Kamseu, E.; Tchamba, A.B.: Laterite based stabilized prodcts for sustainable building applications in tropical countries : review and prospects for the Case of Cameroon. Sustainability **3**, 293–305 (2011). https://doi.org/10.3390/su3010293
29. Nath, S.K.; Maitra, S.; Mukherjee, S.; Kumar, S.: Microstructural and morphological evolution of fly ash based geopolymers. Constr. Build. Mater. **111**, 758–765 (2016). https://doi.org/10.1016/j.conbuildmat.2016.02.106
30. Bewa, C.N.; Tchakouté, H.K.; Rüscher, C.H.; Kamseu, E.; Leonelli, C.: Influence of the curing temperature on the properties of poly (phosphor–ferro–siloxo) networks from laterite. SN Appl. Sci. (2019). https://doi.org/10.1007/s42452-019-0975-5
31. Lemougna, P.N.; Madi, A.B.; Kamseu, E.; Melo, U.C.; Delplancke, M.P.; Rahier, H.: Influence of the processing temperature on the compressive strength of Na activated lateritic soil for building applications. Constr. Build. Mater. **65**, 60–66 (2014). https://doi.org/10.1016/j.conbuildmat.2014.04.100

32. Song, X.J.; Marosszeky, M.; Brungs, M.; Munn, R.: Durability of fly ash based Geopolymer concrete against sulphuric acid attack, In: 10DBMC International Conference on Durability of Building Materials and Components, pp. 17–20 (2005). https://doi.org/10.1049/sqj.1969.0005
33. Das, S.; Yang, P.; Singh, S.S.; Mertens, J.C.E.; Xiao, X.; Chawla, N.; Neithalath, N.: Effective properties of a fly ash geopolymer: Synergistic application of X-ray synchrotron tomography, nanoindentation, and homogenization models. Cem. Concr. Res. **78**, 252–262 (2015). https://doi.org/10.1016/j.cemconres.2015.08.004
34. Ahmari, S.; Zhang, L.: Production of eco-friendly bricks from copper mine tailings through geopolymerization. Constr. Build. Mater. **29**, 323–331 (2012). https://doi.org/10.1016/j.conbuildmat.2011.10.048
35. Tome, S.; Bewa, C.N.; Nana, A.; Deutou Nemaleu, J.G.; Etoh, M.A.; Tchakouté, H.K.; Kumar, S.; Etame, J.: Structural and physico-mechanical investigations of mine tailing-calcined kaolinite based phosphate geopolymer binder. SILICON **14**, 3563–3570 (2022). https://doi.org/10.1007/s12633-021-01137-w
36. Kaze, R.C.; Myllyam, L.; Moungam, B.; Cannio, M.; Rosa, R.; Kamseu, E.; Melo, U.C.; Leonelli, C.: Microstructure and engineering properties of Fe_2O_3(FeO)–Al_2O_3–SiO_2 based geopolymer composites. J. Clean. Prod. **199**, 849–859 (2018). https://doi.org/10.1016/j.jclepro.2018.07.171
37. Giogetti, J.; Nemaleu, D.; Cyriaque, R.; Tome, S.; Alomayri, T.; Assaedi, H.; Kamseu, E.; Chinje, U.; Maria, V.: Powdered banana peel in calcined halloysite replacement on the setting times and engineering properties on the geopolymer binders. Constr. Build. Mater. **279**, 122480 (2021). https://doi.org/10.1016/j.conbuildmat.2021.122480
38. Dhal, N.K.; Muduli, S.D.: Atmospheric Co_2 Sequestration through Mineral Carbonation of Fly Ash, (2016)
39. Kaze, R.C.; Moungam, L.M.B.; Djouka, M.L.F.; Nana, A.; Kamseu, E.; Melo, U.F.C.; Leonelli, C.: The corrosion of kaolinite by iron minerals and the effects on geopolymerization. Appl. Clay Sci. **138**, 48–62 (2017). https://doi.org/10.1016/j.clay.2016.12.040
40. Heah, C.Y.; Kamarudin, H.; Al, A.M.M.; Binhussain, M.: Physics procedia effect of curing profile on kaolin-based geopolymers. Phys. Procedia **22**, 305–311 (2011). https://doi.org/10.1016/j.phpro.2011.11.048
41. Davidovits, J.L Properties of geopolymer cements Joseph davidovits geopolymer institute, 02100 Saint-Quentin, France, pp. 1–19 (1994)